Vol. 13, No. 35, summer 2023, pages 19-30

Journal of Analytical and Numerical Methods in Mining Engineering

Journal home page: http://anm.yazd.ac.ir/

Research article

A plastic analysis of radial displacements at tunnel crown based on the non-associated flow rule

Hamid Mohammadi[1*], Anna Soltani Esmaeili[2]

1- Dept. of Mining Engineering, Vali-e-Asr University of Rafsanjan, Rafsanjan, Iran
2- M.Sc. in Rock Mechanics, & Independent Consultant in Mining and Geotechnical Projects, Rafsanjan, Iran

*Corresponding author: E-mail: *hamid.mohammadi@vru.ac.ir*
(Received: *December 2022*, Accepted: *February 2023)*

DOI: 10.22034/ANM.2023.19335.1583

Keywords

Ground reaction curve
Non-associated flow rule
Dilation angle
Radial displacement

Abstract

This paper considers the non-associated flow rule to propose an analytical solution to calculate the ground reaction curve at the crown of a circular tunnel. This solution is based on the Mohr-Coulomb failure criterion and the dilation angle has been considered as a function of two factors of rock mass quality and confining stress. The results show that if the radial displacements are not controlled, a loosening zone is produced in the tunnel crown (cohesion=0.2 MPa and friction angle=25°). Moreover, based on the trend of the ground reaction curve at the tunnel crown, three new concepts "minimum required support pressure", "maximum allowable strain", and "safety factor based on the maximum allowable strain" was presented. Considering the interaction between the support characteristics curve and ground reaction curves, the efficiency of the associated flow rule to the non-associated flow rule was investigated. Results state that the use of the associated flow rule causes some sort of computational errors in determining the maximum allowable strain (too high) and consequently, the design accuracy of the support system is very low. Moreover, taking into account the associated flow and non-associated flow rules at the sidewall and tunnel crown, the interaction between the support characteristics curve and ground reaction curve was investigated. Based on the results, it was suggested that to design an optimal support system, it is necessary to calculate the safety factor based on the maximum allowable strain by considering the interaction between the support characteristics curve and the ground reaction curve at the tunnel crown. Finally, a procedure was presented for the design of the support system.

1. INTRODUCTION

To study the relationship between induced stresses and displacement fields surrounding underground openings such as tunnels, the understanding stress–strain relation of material (rock or soil) before and after failure and subsequently their mechanical behavior model is very important [1-3]. One of the most important nonlinear responses to the stress–strain behavior of the material, which has an effective role in the value of displacements, is dilatancy. Based on the continuum mechanics, dilatancy is often evaluated by the dilation angle (ψ) [4-7].

The investigation of the previous studies in the tunneling field is shown that the approach of considering the dilation angle is often simplistic; the dilation angle is considered as either one of two values of zero in a non-associated flow rule or the same as the internal friction angle of material in an associated flow rule. But, some researchers

have shown that the application of the associated flow rule and a simple state of the non-associated flow rule (ψ=0) to study the post-failure behavior of the material is not suitable [8-12]. In reality, in the associated flow rule the failure criterion determines both yielding and flow direction (plastic strain rate) simultaneously. However, various studies showed the invalidity of the associated flow rule concept for application to highly anisotropic materials, porous, granular, and geologic materials (rock and soil) has been proven, because large gradients on the curvature of the associated flow rule yield surface may cause convergence problems [13-16]. Spitzig and Richmond [13] showed that the associated flow rule over-predicts the plastic dilatation in the presence of superimposed hydrostatic pressure. Thus, describing the mentioned materials in terms of both plastic strain rate and yielding behavior with an identical criterion for yield criterion and plastic potential function is not proper, and also the associated flow rule is unable to deal with zero plastic dilatancy and pressure sensitivity, because zero plastic dilatancy requires the plastic potential to be a function of the deviatoric stress only, and must therefore be insensitive to pressure [17,18].

Unlike the associated flow rule, the non-associated flow rule is considered two separate functions for yield function (failure criterion) and plastic potential function, so that the yield function describes the elastic limit and the plastic potential function represents the plastic strain rate direction [19]. Therefore, the non-associated flow rule could be applied for an explanation of simultaneous pressure sensitivity and negligible plastic dilatancy. Also, using the non-associated flow rule for the highly anisotropic materials, porous, granular, and geologic materials, the curvature is reduced and consequently, the convergence is improved [18,19].

Recently, some researchers have applied the ground reaction curve (GRC) to investigate the effect of dilatancy on the radial displacements and the interaction between ground and tunnel [8-10,12,20-24]. The trend of GRC depends on the plastic zone radius (R_p) surrounding the tunnel and it has an important role in determining the characteristics support system. In most previous research, generally, the GRC has been calculated for the sidewall (GRC^{wall}) and crown of the tunnel (GRC^{crown}) [8,9,20-29]. It should be noted, due to the effect of plastic weight on the radial displacements, the trend of GRC^{crown} differs from GRC^{wall}. Roussev [29], considering a plastic zone with brittle behavior surrounding a circular tunnel within an infinite rock mass subjected to hydrostatic in situ stress (σ_0) (Fig. 1), showed that, due to the plastic zone weight, if the bearing capacity of support system is low, and it cannot control the radial displacements, the plastic zone radius will be extended and consequently the radial displacements are increased extremely, therefore an ascending part in the trend of GRC^{crown} is produced.

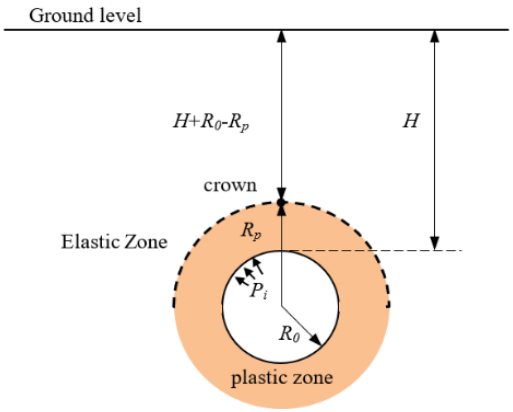

Fig. 1. Plastic zone around a circular tunnel.

However, Roussev [29], to calculate the radial displacements, considered the simplistic approach of the associated flow rule. Based on this rule, the maximum practical value of the dilation angle is assumed to be equal to the internal friction angle which corresponds to the associated plasticity. Therefore, the obtained trend of GRC^{crwon} is unrealistic. In this paper, considering the non-associated rule, the brittle behavior of rock mass, and the effect of plastic zone weight, an analytical solution for calculating GRC^{crown} is presented. Also, in this solution, the amount of ψ is not considered constant but also it is a function of confining stress and rock mass quality. Moreover, based on the trend of GRC^{crown}, three concepts of "minimum required support pressure", "maximum allowable strain", and "safety factor based on the maximum allowable strain" are suggested and finally the effect of dilation angle on the GRC^{crown}, the minimum required support pressure, maximum allowable strain, and the interaction between support system and GRC^{crown} is investigated.

2. CALCULATION OF THE PLASTIC ZONE RADIUS

The process of determining the plastic zone radius requires the utilization of a proper failure criterion (yield function) applicable to the material being considered. In this study, it is assumed that the rock mass around the tunnel satisfies the Mohr-Coulomb failure criterion. In polar coordinates and considering the hydrostatic stress field, the Mohr-Coulomb failure criterion can be written as follows [23]:

$$\sigma_\theta = k\sigma_r + \sigma_{cm}\,,\ k = \frac{1+\sin\phi}{1-\sin\phi}\,,\ \sigma_{cm} = \frac{2c\cos\phi}{1-\sin\phi} \tag{1}$$

where, c is the cohesion of rock mass, φ is the internal friction angle of the rock mass. Moreover, for damaged rock mass, the Mohr-Coulomb failure is rewritten as follows [23]:

$$\sigma_\theta = k'\sigma_r + \sigma'_{cm},\ k' = \frac{1+\sin\phi_r}{1-\sin\phi_r},\ \sigma'_{cm} = \frac{2c_r\cos\phi_r}{1-\sin\phi_r} \tag{2}$$

where, c_r and φ_r are the residual values of cohesion and internal friction angle, respectively.

Eq. (3) is applied to calculate R_p [29]. Therefore, by substituting Eq. (1) into Eq. (3), it yields a differential equation for the stress field within the plastic zone as Eq. (4):

$$\frac{d\sigma_r}{dr} + \frac{\sigma_r - \sigma_\theta}{r} = 0 \tag{3}$$

$$\frac{d\sigma_r}{dr} + \frac{(1-k)\sigma_r - \sigma_{cm}}{r} = 0 \tag{4}$$

Considering the boundary condition at the tunnel circumference (at tunnel radius, R_0, the support pressure is equal to P_{i1}), Eq. (4) can be solved as below:

$$\sigma_r = \frac{-\sigma_{cm}}{k-1} + \frac{r^{k-1}\left(P_{i1} + \frac{\sigma_{cm}}{k-1}\right)}{{R_0}^{k-1}} \tag{5}$$

It should be noted that $P_{i1}\geq 0$. Outside plastic zone, $r\geq R_p$, the radial and tangential stresses are calculated as [30]:

$$\sigma_r = \sigma_0 - \left(\frac{R_p}{r}\right)^2\left(\sigma_0 - \sigma_{r=R_p}\right) \tag{6}$$

$$\sigma_\theta = \sigma_0 + \left(\frac{R_p}{r}\right)^2\left(\sigma_0 - \sigma_{r=R_p}\right) \tag{7}$$

where,$\sigma_{r=R_p}$ is the radial stress at the outer boundary of plastic zone (boundary between elastic zone and plastic zone). Therefore, with considering $r=R_p$, the summation of stresses at the outer boundary of plastic zone yields:

$$\sigma_\theta + \sigma_r = 2\sigma_0 \tag{8}$$

Furthermore, according to Eq. (1), the stress summation at the outer boundary of plastic zone is:

$$\sigma_\theta + \sigma_r = (1+k)\sigma_{r=R_p} + \sigma_{cm} \tag{9}$$

Considering Eq. (8) and Eq. (9),$\sigma_{r=R_p}$can be obtained by solving the following equation:

$$2\sigma_0 = (1+k)\sigma_{r=R_p} + \sigma_{cm} \tag{10}$$

Therefore,

$$\sigma_{r=R_p} = \frac{2\sigma_0 - \sigma_{cm}}{1+k} \tag{11}$$

On other hand, at $r=R_p$, Eq. (5) is written as below:

$$\sigma_{r=R_p} = \frac{-\sigma_{cm}}{k-1} + \frac{{R_p}^{k-1}\left(P_{i1} + \frac{\sigma_{cm}}{k-1}\right)}{{R_0}^{k-1}} \tag{12}$$

Therefore, considering Eq. (11) and Eq. (12), R_p can be obtained by the following equation:

$$R_p = R_0\left(\frac{\left(\frac{2\sigma_0 - \sigma_{cm}}{1+k} + \frac{\sigma_{cm}}{k-1}\right)}{\left(P_{i1} + \frac{\sigma_{cm}}{k-1}\right)}\right)^{\frac{1}{k-1}} \tag{13}$$

3. CALCULATION OF THE PRESSURE DUE TO PLASTIC ZONE WEIGHT

Eq. (14), considering the resistance properties of damaged rock mass within plastic zone, is used to calculate the pressure due to plastic zone weight [29]. Therefore, substituting Eq. (2) into Eq. (14) yields a differential equation within the plastic zone as Eq. (15):

$$\frac{d\sigma_r}{dr} + \frac{\sigma_r - \sigma_\theta}{r} + \gamma = 0 \tag{14}$$

$$\frac{d\sigma_r}{dr} + \frac{(1-k')\sigma_r - \sigma'_{cm}}{r} + \gamma = 0 \tag{15}$$

At the tunnel crown, the radial direction and vertical direction are the same and also the plastic zone weight produces a radial stress in the vertical direction. On the other hand, at the outer boundary of plastic zone, the radial stress due to plastic zone weight is equal to zero. Therefore, by considering the boundary condition at the outer boundary of plastic zone (at R_p, σ_r is equal to zero) Eq. (15) is solved as:

$$\sigma_r = \frac{-\sigma'_{cm}(k'-2) + r\gamma(k'-1)}{(k'-1)(k'-2)} - \left(\frac{{R_p}^{1-k'}}{r^{1-k'}}\right)\left(\frac{-\sigma'_{cm}(k'-2) + R_p\gamma(k'-1)}{(k'-1)(k'-2)}\right) \tag{16}$$

Note that in Eq. (16), while $r=R_0$, the pressure due to the plastic zone weight on the tunnel circumference (P_{i2}) is obtained as follows:

$$P_{i2} = \frac{-\sigma_{cm}^{'}(k^{'}-2)+R_0\gamma(k^{'}-1)}{(k^{'}-1)(k^{'}-2)} - \left(\frac{R_p{}^{1-k^{'}}}{R_0{}^{1-k^{'}}}\right)\left(\frac{-\sigma_{cm}^{'}(k^{'}-2)+R_p\gamma(k^{'}-1)}{(k^{'}-1)(k^{'}-2)}\right) \quad (17)$$

4. CALCULATION OF THE RADIAL DISPLACEMENTS

4. 1. The Elastic Radial Displacements

The rock mass behaviour of outside plastic zone is elastic. Due to the tunnel excavation, the magnitude and orientation of in situ stresses at outside plastic zone change. However, these changes are not significant enough to have influence on the tunnel stability and the rock mass behaviour remains elastic, therefore the type of radial displacements is elastic so that the maximum elastic radial displacement is happened at the outer boundary of plastic zone which obtained by the following equation [31]:

$$u_{r=R_p} = -\frac{(1+\nu)R_p}{E}\left(\sigma_0 - \sigma_{r=R_p}\right) \quad (18)$$

4. 2. The Plastic Radial Displacements

The plastic radial displacements are related to plastic zone. To calculate the plastic radial displacement, at the first step, the maximum plastic zone radius which could be happened must be determined. Roussev [29] showed that if the bearing capacity of support system is not sufficient, and it cannot control the displacements, the plastic radius will be extended extremely and consequently a loosening zone is created around tunnel with radius of $R_{loosening}$. According to Eq. (12), due to the increment of plastic zone radius, the radial stress at the outer boundary of plastic zone is reduced, therefore, from theoretical point of view, the extension of plastic zone radius may be continued until the radial stress at outer boundary is larger than zero [29]. Thus, by substituting $\sigma_0=\gamma(H+R_0-R_p)$ in Eq. (11), $R_{loosening}$ can be found based on Eq. (19). It should be noted that, in reality, $R_{loosening}$ may be appeared at less value than the value obtained from Eq. (19) [29]. It should be noted that when P_{i1} is zero, the loosening zone can be created. Moreover, to calculate P_{i2}, R_p changes within the range of R_0 and $R_{loosening}$.

$$R_{loosening} = H + R_0 - \frac{2c\cos\phi}{2\gamma(1-\sin\phi)} \quad (19)$$

It should be noted that, to calculate the plastic radial displacement, R_p changes within the range of R_0 and $R_{loosening}$. Within plastic zone, the total strain is obtained by sum of elastic and plastic strains as follows:

$$\varepsilon_r = \varepsilon_r^{elastic} + \varepsilon_r^{plastic} \quad (20)$$

$$\varepsilon_\theta = \varepsilon_\theta^{elastic} + \varepsilon_\theta^{plastic} \quad (21)$$

where ε_r is the radial strain, ε_θ is the tangential strain. Considering axisymmetric conditions, the relationships between strain and radial displacement (u_r) at any point in the material define accordance Eqs. (22) and (23). It should be noted that compressive direct strains and radially outward displacements take in to positive.

$$\varepsilon_r = -\frac{du_r}{dr} \quad (22)$$

$$\varepsilon_\theta = -\frac{u_r}{r} \quad (23)$$

To determine the strain field in plastic zone, a plastic flow rule is needed which in this research, based on the mentioned advantages and disadvantages for flow rules in the introduction, the non-associated flow rule was considered. In the non-associated flow, separately, the limit between elastic and non-elastic is described by the failure criterion and the plastic potential function represents the plastic strain rate direction [19]. Thus, the plastic potential function is as follows [23]:

$$f(\sigma_r,\sigma_\theta) = \sigma_\theta - K_\psi\sigma_r - 2c\sqrt{K_\psi} = 0 \quad (24)$$

A review of a number of publications on this topic reveals that, to calculate K_ψ, the dilation angle is considered as a constant value, whereas, some researchers [5,10,32] showed the use of a constant dilation angle in calculation process of displacements is an unrealistic and misleading analysis. Based on the experimental results of triaxial compression tests, it is shown that the dilation angle is a function of plastic parameters and confining stress so that, the dilation angle gradually decreased with increasing confining stress [10, 33-35]. Alejano and Alonso [10] to consider the effects of confining stress plastic parameters, presented a new model based on the experimental tests, for calculating the actual dilatancy and showed that both factors of the quality of the rock mass and confining stress affect on the actual dilatancy values. Finally, they presented an empirical relationship to calculate the peak value of dilation angle as follows:

$$\psi_{peak} = \frac{\phi}{1+log_{10}\sigma_{ci}} log\frac{\sigma_{ci}}{\sigma_3+0.1} \quad (25)$$

where, σ_{ci} is the uniaxial compressive strength of intact rock and σ_3 is the confining stress.

Alejano and Alonso [10] investigated the dilatancy decay to the plastic parameters and suggested the Eq. (26) to calculate K_ψ. In studying decay in the dilatancy angle in line with plasticity, the first option is to assign an exponential decay function to K_ψ (the dilatancy relationship). The decay goes from a previously estimated peak value to a null value corresponding to no plastic volume increase. This null value is proposed in the light of the fact that a rock cannot dilate infinitely.

$$K_\psi = 1 + (K_{\psi,peak} - 1)e^{\frac{-\eta}{\eta^*}} \tag{26}$$

$$K_{\psi,peak} = \frac{1 + sin\,\psi_{peak}}{1 - sin\,\psi_{peak}} \tag{27}$$

The parameter η^* is the plastic parameter which marks the transition to residual strength values which, for brittle behaviour, is obtained as Eq. (28) and η is defined as the difference between the major and minor principal plastic strains, which reflects the plastic shear strain. It should be noted that in the elastic–brittle–plastic behaviour model, there is a sudden loss of strength, therefore for brittle rocks, the values of η and η* are the same [10].

$$\eta^* = \left[\frac{\sigma_\theta^{peak}(\sigma_r) - \sigma_\theta^{res}(\sigma_r)}{E}\right](1 + K_\psi) \tag{28}$$

The non-elastic parts of radial and tangential strains may be related to the plane strain condition as follows [36]:

$$\varepsilon_r^{plastic} = -K_\psi \varepsilon_\theta^{elastic} \tag{29}$$

With considering Eqs. (20)-(30) the differential equation of radial displacement is obtained as follows:

$$\frac{du_r}{dr} + K_\psi \frac{u_r}{r} = f(r) \tag{30}$$

where

$$f(r) = \varepsilon_r^{elastic} + K_\psi \varepsilon_\theta^{elastic} \tag{31}$$

Thus, the radial displacement at elastic-plastic interface can be calculated by solving Eq. (32). It should be noted that the Eq. (18) is applied as the boundary condition of Eq. (32) [8].

$$u_r = r^{-K_\psi}\int_{R_p}^{r} r^{K_\psi} f(r)dr + u_{r=R_p}\left(\frac{R_p}{r}\right)^{K_\psi} \tag{32}$$

where E is the Young's modulus and ν is the poisson's ratio of the material.

According to Eq. (31), $f(r)$ is a function of elastic strains; hence to calculate Eq. (32), the values of elastic strains are needed. Eqs. (33) and (34) are expressions for the radial and tangential strains in elastic zone.

$$\varepsilon_r^{elastic} = \frac{(1+\nu)}{E}\left((1 - 2\nu)\left(\frac{\left(\sigma_{r=R_p} - \sigma_0\right)R_p^2 - (P_{i1} + P_{i2} - \sigma_0)R_0^2}{R_p^2 - R_0^2}\right) + \frac{\left(P_{i1} + P_{i2} - \sigma_{r=R_p}\right)R_0^2 R_p^2}{r^2\left(R_p^2 - R_0^2\right)}\right) \tag{33}$$

$$\varepsilon_\theta^{elastic} = \frac{(1+\nu)}{E}\left((1 - 2\nu)\left(\frac{\left(\sigma_{r=R_p} - \sigma_0\right)R_p^2 - (P_{i1} + P_{i2} - \sigma_0)R_0^2}{R_p^2 - R_0^2}\right) - \frac{\left(P_{i1} + P_{i2} - \sigma_{r=R_p}\right)R_0^2 R_p^2}{r^2\left(R_p^2 - R_0^2\right)}\right) \tag{34}$$

Therefore

$$f(r) = \frac{(1+\nu)}{E}\left(\begin{array}{c}(1-2\nu)(1+K_\psi)\\ \left(\frac{\left(\sigma_{r=R_p} - \sigma_0\right)R_p^2 - (P_{i1} + P_{i2} - \sigma_0)R_0^2}{R_p^2 - R_0^2}\right) + \\ (1 - K_\psi)\left(\frac{\left(P_{i1} + P_{i2} - \sigma_{r=R_p}\right)R_0^2 R_p^2}{r^2\left(R_p^2 - R_0^2\right)}\right)\end{array}\right) \tag{35}$$

Consequently, the analytical expression of the radial displacement within plastic zone is derived by integrating Eq. (32) as Eq. (36), which with replacing $r=R_0$, into Eq. (36), the radial displacement at the tunnel circumference can be determined. It should be noted that to apply the associated flow rule to determine the radial displacement, new equations can be derived by substituting the internal friction angle for the dilation angle in Eq. (36) which used in the non-associated flow rule [23].

$$u_r = \frac{(1+\nu)}{E} R_0^{-K_\psi} \left(\begin{array}{c} \left(\frac{\left(\sigma_{r=R_p} - \sigma_0\right) R_p^2 - (P_{i1} + P_{i2} - \sigma_0) R_0^2}{R_p^2 - R_0^2} \right) \\ (1-2\nu)\left(R_p^{K_\psi+1} - r^{K_\psi+1}\right) \\ - \left(\frac{\left(P_{i1} + P_{i2} - \sigma_{r=R_p}\right) R_0^2 R_p^2}{R_p^2 - R_0^2} \right) \\ \left(R_p^{K_\psi-1} - r^{K_\psi-1}\right) \end{array} \right) - \frac{(1+\nu) R_p}{E} \left(\sigma_0 - \sigma_{r=R_p}\right) \left(\frac{R_p}{r}\right)^{K_\psi} \quad (36)$$

5. EVALUATION OF THE SUGGESTED SOLUTION

In order to evaluate the analytical solution, A circular tunnel with a radius of 5 m and a depth of 100 m is considered. The rock mass properties are given in Table 1. According to Fig. 2, GRC^{crown} was obtained based on the suggested solution and compared with the Roussev results. It should be noted, in this research, for calculating GRC^{crown}, the absolute value of radial displacement was considered. As shown in Fig. 2, the calculated GRC^{crown} by the suggested solution is in good agreement with the Roussev results, which show the ability of the suggested solution. It should be noted that in the Roussev method [29], the radial displacements were calculated based on the associated flow rule, thus, to evaluate, it was assumed that the dilation angle is equal to the internal friction angle of the rock mass.

Table 1. Input data to investigate the performance of suggested solution

γ (MN/m³)	E (MPa)	ν	c (MPa)	φ (°)	c_r (MPa)	φ_r (°)
0.024	450	0.32	0.2	25	0.02	11.5

In Fig. 3, considering the non-associated flow rule and a variable value for dilation angle, the trend of GRC^{crown} has been compared with the Roussev method. Based on the Eq. (25), the maximum dilation angle is about 13.5°, while considering the associated flow rule, the amount of dilation angle is constant and equal to 25°. Therefore, the trend of GRC^{crown} is very different compared to the Roussev method. Moreover, in Fig.3, based on the suggested solution, GRC^{crown} was compared with GRC^{wall}, which will be explained in the next section.

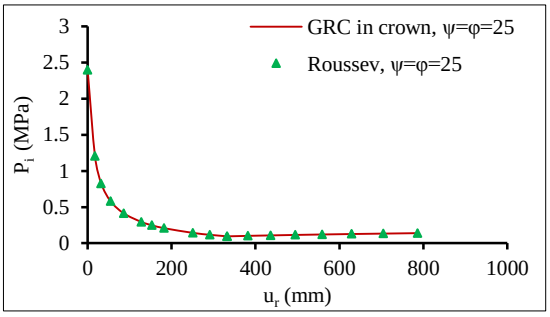

Fig. 2. Comparison of GRC^{crown} based on suggested solution and Roussev method [29] considering the associated flow rule.

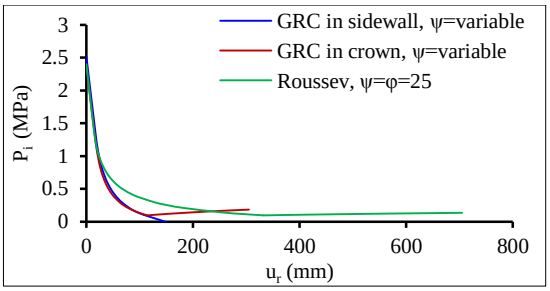

Fig. 3. Comparison between trends of GRC^{crown} and GRC^{wall} considering the non-associated flow rule.

6. THE DIFFERENCE BETWEEN GRC^{CROWN} AND GRC^{WALL}

In order to describe the properties of GRC^{crown}, a typical view of GRC^{crown} and GRC^{wall} is shown in Fig. 4. According to this figure, GRC^{crown} is consisted of two parts; 1) the descending part which consists of an elastic part (from point A to point B) and a non-elastic or plastic part (from point B to point C), and 2) the ascending part which consists of a non-elastic part with loosening behavior (from point C to point D). Therefore, before point C, the plastic zone has not been loosened and after point C, this zone has been loosened and consequently the tunnel collapses. In reality, when the loosening zone is produced, a highly damaged zone will be created in the surrounding of the tunnel. Point D shows the ultimate radial displacement which is due to the loosening zone radius.

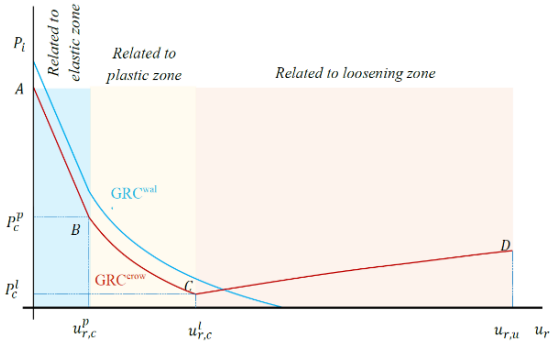

Fig. 4. A typical view of GRC^{crown} and GRC^{wall}.

However, GRC^{wall} is only consisted of the descending part which consists of an elastic part and a plastic part, and the maximum radial displacement occurs when the support pressure is zero. Therefore, the trend of GRC^{crown} is different from GRC^{wall}, and based on it, three new concepts of "minimum required support pressure", "maximum allowable strain", and "safety factor based on the allowable strain" have been obtained, which the first two concepts are introduced below, and the third concept is introduced in section 7.

a. Minimum required support pressure ($P_{s,min}$):

Point C is a turning-point for GRC^{crown}, so that beyond the C, the loosening zone is created and the tunnel may be completely unstable. The active pressure at C is named "critical loosening pressure" (P_c^l). Therefore, to prevent the creation of loosening zone, the minimum required support pressure is equal to the critical loosening pressure, which can be calculated as below:

$$P_{s,min}=\frac{-\sigma_{cm}'(k'-2)+R_0\gamma(k'-1)}{(k'-1)(k'-2)} - \left(\frac{R_p^c}{R_0}\right)^{1-k'}\left(\frac{-\sigma_{cm}'(k'-2)+R_p^c\gamma(k'-1)}{(k'-1)(k'-2)}\right) \quad (37)$$

where,R_p^c is the plastic zone radius at the point C and obtained from Eq. (15), when P_{i1}=0.

b. Maximum allowable strain (ε_{all}):

The maximum allowable strain is equal to the maximum strain that can occur prior to the loosening zone is created. Therefore, to prevent the creation of loosening zone, the interaction strain between the support system and ground must be less than the maximum allowable strain. The maximum allowable strain is defined as below:

$$\varepsilon_{all}=\frac{u_{r,c}}{R_0}=\frac{u_{r,c}^l}{R_0} \quad (38)$$

where,$u_{r,c}^l$ is critical loosening radial displacement that can be obtained from Eq. (36) while $r=R_p^c$.

7. INVESTIGATION OF DILATANCY EFFECT

As before mentioned, the actual dilatancy value is a function of both factors of the rock mass quality and confining stress [10]. For calculating the peak dilation angle based on the Eq. (25), the confining stress (σ_3) is equal to the radial stress at the outer boundary of plastic zone ($\sigma_3=\sigma_{r=R_p}$). Figs. 5-8 show an evaluation of the relationship between dilation angle and the plastic radius, confining stress, radial displacement, and maximum allowable strain. As shown in Figs. 5 and 6, with increasing the plastic zone radius and decreasing the confining stress, the dilation angle is increased non-linearly. It should be noted that, based on the Eq. (12) with increasing the plastic zone radius, the confining stress is decreased. Eqs. (12) and (13) show that the radial stress at the outer boundary of plastic zone and the plastic radius are independent of dilation angle. Also, based on the Eq. (25), the dilation angle is a function of the radial stress at the outer boundary of plastic zone (confining stress). In Fig. 9, taking into account the associated and non-associated flow rules, the relationship between the plastic zone radius and the radial displacement has been investigated.

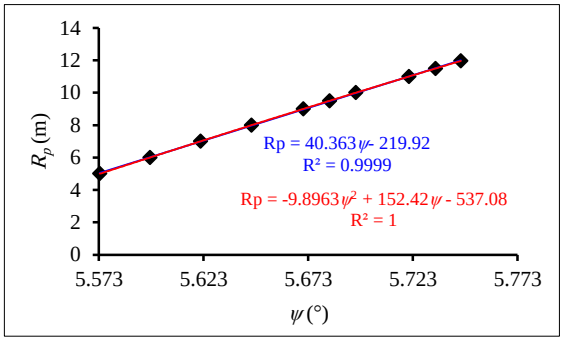

Fig. 5. Relationship between the plastic zone radius and dilation angle.

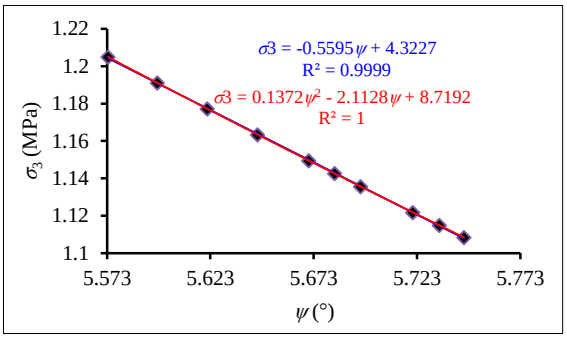

Fig. 6. Relationship between the confining stress and dilation angle.

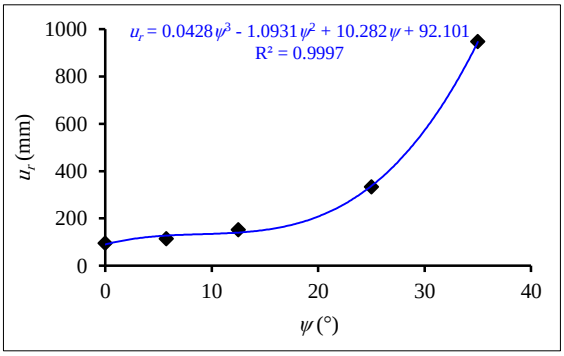

Fig. 7. Relationship between the radial displacement and dilation angle.

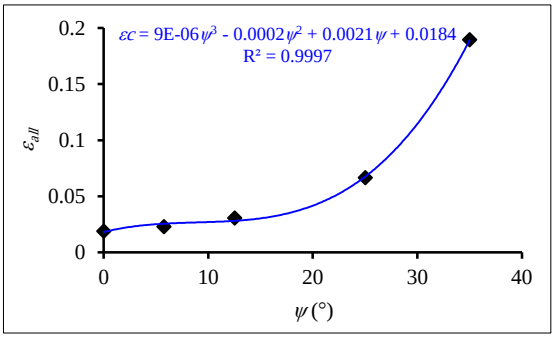

Fig. 8. Relationship between the maximum allowable strain and dilation angle.

As shown in this figure, at the same plastic zone radius, the obtained radial displacements from the associated flow rule are greater than the obtained radial displacements from the non-associated flow rule. In Fig. 10, considering the non-associated flow rule, the GRC^{crown} has been calculated and compared with the obtained GRC^{crown} from the associated flow rule.

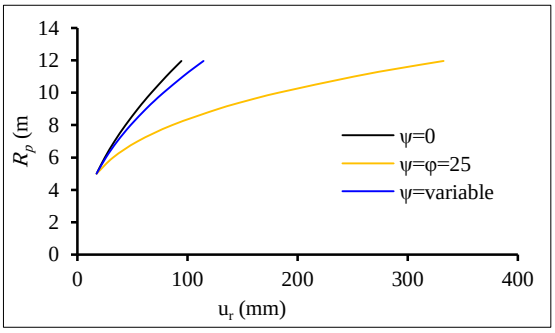

Fig. 9. Influence of dilation angle on the relation between plastic zone radius and radial displacement.

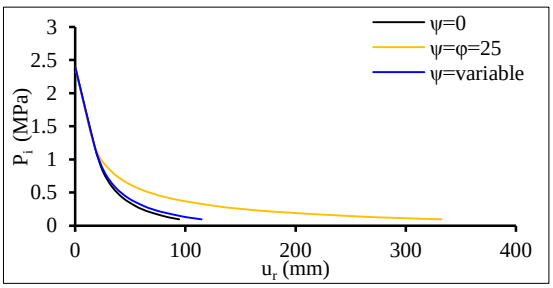

Fig. 10. Influence of dilation angle on the GRC^{crown}.

According to Eqs. (37) and (38) the values of minimum required support pressure and maximum allowable strain depends on the location of turning-point C at the GRC^{crown} in Fig. 4. As shown in Fig. 10, the place of point C is a function of the type of plastic potential function so that, when the non-associated flow rule is considered (ψ is variable), the dilation angle is always less than the internal friction angle of rock mass, thus the place of point C at the obtained GRC^{crown} from the non-associated flow rule is always behind point C at the obtained GRC^{crown} from the associated flow rule. In Table 2, the properties of point C for two conditions of the associated flow rule and non-associated flow rule have been compared. Moreover, in Table 3, considering the effect of non-associated flow rule, the reduction percent for each of properties of point C have been calculated and compared with the associated flow rule condition. According this Table, the reduction of maximum allowable strain is equal to 65% whereas due to independence the minimum required support pressure from the dilation angle, the value of $P_{s,min}$ is constant.

In order to demonstrate the performance of the non-associated flow rule to calculate the radial displacements, it must be used the concept of interaction between the support system and tunnel. Therefore, four support systems are considered. As shown in Table 4, the support systems are the same from a resistance point of view (maximum bearing capacity ($P_{s,max}$) and stiffness (K_s)) and the only difference is related to the initial displacement of the tunnel which occurs before the support installation (u_{r0}). There are two questions; first, why should the support be designed considering the interaction between the support characteristics curve (SCC) and obtained GRC from the non-associated flow rule? And second, why can't GRCwall be used for support design when the loosening zone is created? To answer these questions, the interaction between SCC with different trends GRC^{wall} is shown in Fig. 11 and its results are mentioned in Table 5.

Table 2. Properties of point C

Description	Associated flow rule	Non-associated flow rule (ψ is constant)	Non-associated flow rule (ψ is variable)
$P_{s,min}$ (MPa)	0.1	0.1	0.1
ε_{all} (%)	6.6	1.8	2.3
u_r (mm)	332	94	114
ψ_{peak}° (deg.)	25	0	13.5
ψ°	25	0	5.7
R_p (m)	11.9	11.9	11.9

Table 3. Changes (Δ) of properties point C considering the non-associated

ΔR_p (%)	$\Delta\psi$ (%)	$\Delta\psi_{peak}$ (%)	Δu_r (%)	$\Delta\varepsilon_{all}$ (%)	$\Delta P_{s,min}$ (%)
0	-77	46	-65	-65	0

Table 4. Characteristics of support systems

Support No.	$P_{s,max}$, (MPa)	K_s, (MN/m³)	u_{r0}, (mm)
1	1	25	20
2	1	25	100
3	1	25	140
4	1	25	250

As shown in Fig. 11, when GRC^{wall} is obtained based on the associated flow rule, it is possible to install all the support systems with the aim of achieving a safety factor of larger than 1 (Table 4). Of course, the support 1 is under more pressure compared to support 4, and on the other hand, during the installation of support 4, there is an initial displacement of 250 mm, which is not desirable. In GRC^{wall}, the radial displacements reach their maximum value at P_i=0, whereas, there is no prediction of collapse and the creation of a loosening zone, which is not consistent with reality. The safety factor based on the $P_{s,Max}$ cab be calculated as follows:

$$SF_P = \frac{P_{s,Max}}{P_{int}} \quad (39)$$

where,P_{int} is interaction pressure between SCC and GRC^{wall} or GRC^{crown}.

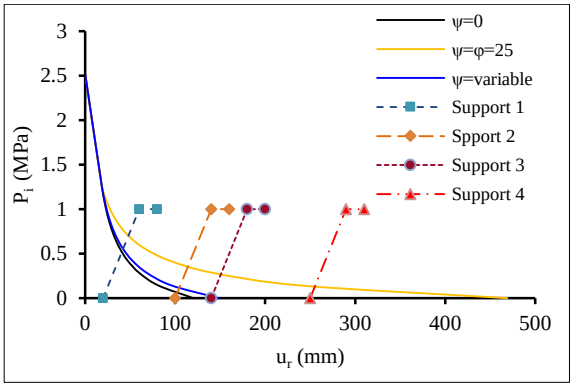

Fig. 11. Interaction between SCC and the descending part of GRC^{wall}.

Table 5. Results of interaction between SCC and GRC^{wall}

Support *No.*	ψ°	P_{int} *(MPa)*	$u_{r,int}$ *(mm)*	ε_{int} *(%)*	SF_P
1	0	0.52	41	0.82	1.92
	variable	0.55	42	0.84	1.81
	25	0.7	48	0.96	1.43
2	0	0.06	103	2.06	16.66
	variable	0.11	105	2.1	9.09
	25	0.35	114	2.28	2.86
3	0	support has no reaction			
	variable	0.03	141	2.82	33.33
	25	0.27	151	3.02	3.70
4	0	support has no reaction			
	variable	support has no reaction			
	25	0.13	255	5.1	7.69

If the GRC^{wall} is considered based on the non-associated flow rule and ψ=0, only the supports 1 and 2 can be installed. In this condition, the GRC^{wall} is very conservative because considering the ψ=0 does not correspond to reality. But, considering the non-associated flow rule and ψ=variable, the supports 1, 2, and 3 can be installed (Fig. 11). However, it should be noted that even considering the non-associated flow rule, the GRC^{wall} does not have the ability to detect the loosening zone, and therefore the support design is not correct. In this situation, it is necessary to use the GRC^{crown} for the support design.

As before mentioned, to prevent of tunnel collapse, the interaction between support system and the rock mass surrounding tunnel must be occurred before the point C at GRC^{crown} (the descending part of GRC^{crown}). Fig. 12 shows that the interaction between the SCC and the descending part of GRC^{crown}. According to this figure, when the GRC^{crown} is calculated based on the associated flow rule, due to large dilation angle (ψ=φ), the dilatancy within the rock mass is very high and consequently, the radial displacements

corresponding to the point C (R_p^C), the radial displacements are greater than the obtained radial displacements from the non-associated flow rule (the plastic zone radius is independent of the dilation angle, thus R_p^C remains constant). In reality, when the radial displacements are calculated based on the associated flow rule, designer can install the support system with a further delay whereas the values of obtaining radial displacements based on the non-associated flow rule are closer to reality.

With considering the obtained GRC^{crown} from the associated flow rule, it is possible to install all the support systems with the aim of achieving a safety factor of larger than 1 (Table 5), whereas, if the support is designed based on the obtained GRC^{crown} from the non-associated flow rule (in condition of ψ is variable), only the supports 1 and 2 can be installed (Fig. 12). Therefore, the design of support system based on the obtained GRC^{crown} from the associated flow rule is accompanied by a significant error and should be avoided. It should be noted that, considering ψ=0, the GRC^{crown} is very conservative, and the design support is not accurate.

As shown in Fig. 12 and Table 6, considering the non-associated flow rule and ψ=variable, there are two choices for the design of the support system; support systems 1 and 2. The SF_P is greater than 1 for both support systems 1 and 2, which are 1.92 and 5.5, respectively. To choose the most optimal support system, a new concept of "safety factor based on the maximum allowable strain " can be used. It is calculated as follow:

c. Safety factor based on the maximum allowable strain (SF_ε):

$$SF_\varepsilon = \frac{\varepsilon_{all}}{\varepsilon_{int}} \qquad (40)$$

Where,ε_{int} is interaction strain between SCC and GRC^{crown}.

When SF_ε =1, it means that the interaction place between SCC and GRC^{crown} coincides with the point C in Fig. 4. Moreover, it indicates that the loosening zone is creating and the support system may not be effective despite the value of SF_P is much greater than 1. When SF_ε is much greater than 1, the possibility of creating a loosening zone is very low.

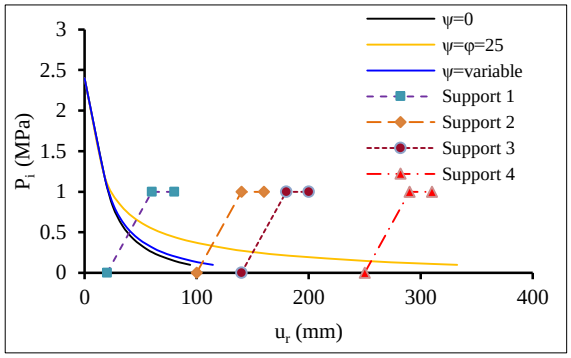

Fig. 12. Interaction of between SCC and the descending part of GRC^{crown}.

Table 6. Results of interaction between SCC and GRC^{crown}

Support No.	ψ°	P_{int} (MPa)	$u_{r,int}$ (mm)	ε_{int} (%)	SF_P	SF_ε
1	0	0.47	39	0.78	2.13	2.3
	variable	0.52	41	0.82	1.92	2.8
	25	0.66	46	0.92	1.51	7.17
2	0	The loosening zone has been created.				
	variable	0.18	105	2.1	5.5	1.1
	25	0.33	114	2.3	3.03	2.9
3	0	The loosening zone has been created.				
	variable	The loosening zone has been created.				
	25	0.26	150	3	3.85	2.2
4	0	The loosening zone has been created.				
	variable	The loosening zone has been created.				
	25	0.14	256	5.1	7.14	1.3

The value of SF_ε is completely dependent on the time and place of support system installation. For example, as shown in Table 6, the only difference between support systems 1 and 2 is the amount of initial displacement at the time of installation, which causes the SF_ε of support 1 to be 155% greater than SF_ε support 2, whereas, the SF_P of support 2 is 186% greater than the SF_P of support 1.

Therefore, the following procedure is suggested to design the support system:

1. It should be checked whether there is a possibility of creating a loosening zone at the tunnel crown or not.

2. If the loosening zone is not created, the GRC^{wall} should be used for support design, and otherwise, the support design should be based on the GRC^{crown}.

3. If the loosening zone is created, it must be calculated the minimum required support pressure and maximum allowable strain.

4. For an optimal design, the SF_P and SF_ε must be calculated and their values checked technically.

8. CONCLUSIONS

In this paper, considering the non-associated flow rule and the effect of plastic zone weight, an analytical solution was presented for calculating GRC^{crown} in circular tunnels. It was also shown that the creation of the loosening zone is possible only at the tunnel crown, and the displacements in the tunnel wall reach their maximum value at the support pressure equal to zero, while at the tunnel crown, due to the creation of the loosening zone, the displacements increase.

The obtained results showed that the dilation angle significantly affects the trend of GRCcrown, so if its value is not chosen correctly, the characteristics of the loosening zone are calculated incorrectly, and as a result, it is not possible to design an optimum support system.

Also, three new concepts of "minimum required support pressure", "maximum allowable strain", and "safety factor based on the maximum allowable strain" were presented and showed that they are very essential in the analysis of tunnel stability. In fact, considering the value of the variable dilation angle, if the loosening zone is created at the tunnel crown, all three mentioned concepts should be taken into account in the design of the support system.

A sensitivity analysis was carried out, which showed that, the determination of radial displacements surrounding the tunnel and consequently GRC^{crown} based on the associated flow rule is wrong. Finally, a design support procedure was suggested and showed that to the design of support system, the calculation of a new concept of "safety factor based on the maximum allowable strain" is required.

Finally, it is suggested that the method of this paper be developed for the non-hydrostatic stress field.

REFERENCES

[1] Nikadat, N., Fatehi, M. and Abdollahipour, A. (2015). Numerical modelling of stress analysis around rectangular tunnels with large discontinuities (fault) by a hybridized indirect BEM. Journal of Central South University, 22: 4291–4299.

[2] Nikadat, N. and Fatehi Marji, M. (2016). Analysis of stress distribution around tunnels by hybridized FSM and DDM considering the influences of joints parameters. Geomechanics and Engineering, 11, 2: 269-288

[3] Lazemi, H.A., Marji, M.F., Bafghi, A.R.Y. and Goshtasbi, K. (2013). Rock failure analysis of the broken zone around a circular opening. Archives of Mining Sciences, 58,1: 165-188

[4] Vermeer, P.A. and Borst, R. (2010). Non-associated plasticity for soils, concrete and rock. Heron, 29(3):1–64.

[5] Zhao, X.G. and Cai, M. (2010). A mobilized dilation angle model for rocks. Int. J. Rock Mech. Min. Sci., 47:368–384.

[6] Bagheri, B., Soltani, F. and Mohammadi, H. (2014). Prediction of plastic zone size around circular tunnels in non-hydrostatic stress field, International Journal of Mining Science and Technology, 4, 1: 81-85.

[7] Han, U.C., Choe, C.S., Hong,K.U. and Pak C. (2022). Prediction of final displacement of tunnels in time-dependent rock mass based on the nonequidistant grey verhulst model, https://doi.org/10.1155/2022/3241171

[8] Yi, K., Kang, H., Ju, W., Liu, Y. and Lu, Z. (2020). Synergistic effect of strain softening and dilatancy in deep tunnel analysis. Tunnell. Undergr. Space Technol., https://doi.org/10.1016/j.tust.2020.103280.

[9] Sharan, S.K. (2005). Exact and approximate solutions for displacements around circular openings in elastic–brittle–plastic Hoek–Brown rock. Int. J. Rock Mech. Min. Sci., 42:542–549.

[10] Alejano, L.R. and Alonso, E. (2005). Considerations of the dilatancy angle in rocks and rock masses. Int. J. Rock Mech. Min. Sci., 42:481–507.

[11] Zhao, X.G. and Cai, M. (2010). Influence of plastic shear strain and confinement-dependent rock dilation on rock failure and displacement near an excavation boundary. Int. J. Rock Mech. Min. Sci., 47:723–738.

[12] Serrano, A., Olalla, C. and Reig, I. (2011). Convergence of circular tunnels in elastoplastic rock masses with non-linear failure criteria and non-associated flow laws. Int. J. Rock Mech. Min. Sci., 48:878–887.

[13] Spitzig, W.A. and Richmond, O. (1984). The effect of pressure on the flow-stress of metals. Acta metal., 32:457-463.

[14] Yoon, J.W., Stoughton, T.B. and Dick, R.E. (2007). Earing prediction in cup drawing based on non-associated flow rule. in: CeasarDeSa, J.M.A., Santos, A.D. (Eds.), Materials Processing and Design: Modeling, Simulation and Applications, Pts I and II. Amer. Inst. Physics, Melville, 685-690.

[15] Cvitanic, V., Vlak, F. and Lozina, Z. (2008). A finite element formulation based on non-associated plasticity for sheet metal forming. Int. J. Plasticity, 24:646-687.

[16] Park, T. and Chung, K. (2012). Non-associated flow rule with symmetric stiffness modulus for isotropic-kinematic hardening and its application for earing in circular cup drawing. Int. J. Solids Struct., 3582-3593.

[17] Stoughton, T.B. (2002). A non-associated flow rule for sheet metal forming. Int. J. Plasticity, 8:687-714.

[18] Stoughton, T.B. and Yoon, J.W. (2006). Review of Drucker's postulate and the issue of plastic stability in metal forming. Int. J. Plasticity, 22:391-433.

[19] Safaei, M. (2013). Constitutive Modelling of Anisotropic Sheet Metals Based on a Non-Associated Flow Rule. PhD thesis, Ghent University.

[20] Brown, E.T., Bray, J.W., Landanyi, B. and Hoek, E. (1983). Ground response curves for rock tunnels. J. Geothech. Eng., 109:15–39.

[21] Carranza-Torres, C. and Fairhurst, C. (2000). Application of the convergence-confinement method of tunnel design to rock masses that satisfy the Hoek–Brown failure criterion. Tunnell. Undergr. Space Technol., 5(2):187–213.

[22] Ghorbani, A. and Hasanzadehshooiili, H. (2019). A comprehensive solution for the calculation of ground reaction curve in the crown and sidewalls of circular tunnels in the elastic-plastic-EDZ rock mass considering strain softening. Tunnell. Undergr. Space Technol., 84:413–431.

[23] Zhang, Q., Li, Y.J., Wang H.Y., Yin, Q. and Wang, X.F. (2022). Re-profiling response of heavily squeezed tunnels via ground reaction curves. Tunnell. Undergr. Space Technol., https://doi.org/10.1016/j.tust.2022.104411.

[24] Park, K.H., Tontavanich, B. and Lee. J.G. (2008). A simple procedure for ground response curve of circular tunnel in elastic–strain softening rock masses. Tunnell. Undergr. Space Technol., 23(2):151–159.

[25] Pacher, F. (1964). Deformationsmessungen in Versuchsstollenals Mittel zur Erforschung des Gebirgsverhaltens und zur Bemessung des Ausbaues. Felsmechanik und Ingenieursgeologie Supplementum, IV:149–161.

[26] Detournay, E. The effect of gravity on the stability of a deep tunnel. Int. J. Rock Mech. Min. Sci., 21(6):349–351.

[27] Hoek, E. and Brown, E.T. (1980). Underground excavations in rock. The Institution of Mining and Metallurgy, London, 1980.

[28] Goodman, R. (1989). Introduction to rock mechanics. John Wiley & Sons.

[29] Roussev, P. (1998). Calculation of the displacements and Pacher's rock pressure curve by the associative law for the fluidity-plastic flow. Tunnell. Undergr. Space Technol. 13(4): 441–451.

[30] Timoshenko, S.P. and Goodier, J.N. (1969). Theory of elasticity. McGraw-Hill Book Co Inc, New York.

[31] Brady, B.H.G. and Brown, E.T. (1993). Rock mechanics for underground mining. London: Chapman & Hall.

[32] Detournay, E. (1986). Elastoplastic model of a deep tunnel for a rock with variable dilatancy. Rock Mech. Rock Eng., 9(2):99–108.

[33] Scholz, C.H. (1968). Microfracturing and the inelastic deformation of rock in compression. J. Geophys. Res., 73(4):1417–32.

[34] Schock, R.N., Heard, H.C. and Stephens, D.R. (1973). Stress–strain behaviour of a granodiorite and two graywackes on compression to 20 kilobars. J. Geophys. Res., 78(26):5922–41.

[35] Be´uelle, P., Desrues, J. and Raynaud, S. (2000). Experimental characterisation of the localisation phenomenon inside a Vosges sandstone in a triaxial cell. Int. J. Rock Mech. Min. Sci., 37(8):1223–37.

[36] Wang, Y. (1996). Ground response of circular tunnel in poorly consolidated rock. J. Geotech. Eng., 122;703–708.